Catalysis Today 172 (2011) 2–7

Contents lists available at ScienceDirect

Catalysis Today

journal homepage: www.elsevier.com/locate/cattod

Catalytic activity of Pt and Pd catalysts supported on HWP/HMS in the selective hydroisomerization of *n*-pentane. Effect of reaction temperature

L. Belandria, N. Marín-Astorga[1], E. García, E. Sosa, F. Aguirre, M. Villarroel, A. Uzcátegui, F. Imbert*

Laboratorio de Cinética y Catálisis, Departamento de Química, Facultad de Ciencias Núcleo "Pedro Rincón Gutiérrez", Universidad de Los Andes, La Hechicera Mérida – Edo, Mérida 5101, Venezuela

ARTICLE INFO

Article history:
Received 1 December 2010
Received in revised form 20 April 2011
Accepted 21 April 2011
Available online 1 June 2011

Keywords:
Hydroisomerization
n-Pentane
HMS
Pt
Pd
HPW

ABSTRACT

Non order structure type HMS was synthesized through a S°I° mechanism. These solids were modified by incorporation of acid (30 wt.% of tungstophosphoric acid) and metallic sites (1% of metal: Pt or Pd), and tested in the hydroisomerization reaction of *n*-pentane. The catalysts were characterized by X-ray diffraction (XRD), N_2 adsorption and desorption, chemisorption of H_2, scanning electron microscopy (SEM), thermogravimetric analysis (TGA) and differential scanning calorimetry (DSC). For the catalyst containing Pt, the effect of reaction temperature was investigated in the range of 200–400 °C, the optimal catalytic activity was reached at 350 °C. The Pt catalyst showed higher conversion, iso-pentane yield and catalytic stability than its Pd counterpart.

1. Introduction

In the 90s, ordered mesostructured materials such as M41S, HMS, and MSU were synthesized [1–5]. Since then, numerous synthesis methods have been developed, using a variety of supramolecular templates to obtain organic, inorganic and/or hybrid mesostructures with a wide range of structural properties, pore sizes, morphologies and surfaces [6]. The ordered mesoporous materials due to their pore diameters can overcome the disadvantage of zeolites [7], since they can host metallic and acid catalytic sites within a larger volume where the transformation of much larger molecules is possible. These materials have pore diameters of 20–500 Å, surface area > 700 m^2/g and pore volume > 0.6 cm^3/g.

Pinnavaia et al. [4,5] have introduced a templating route for preparing mesoporous molecular sieve based on hydrogen-bonding interactions and self-assembly between either S°I° or N°I°, where I° is the inorganic precursor (typically an alkoxide) and S° or N° is the surfactant (typically an amine or a nonionic PEO-based surfactant, respectively). These pathways normally afford mesostructures with wormholelike framework structures. HMS [4] and MSU-X [5] silicas assembled from electrically neutral amines and nonionic di- and triblock surfactants, respectively, are examples of wormhole framework mesostructures. The S°I° templating pathway produces ordered mesoporous materials with thicker framework walls, smaller X-ray scattering domain sizes, and substantially improved textural mesoporosities.

The *n*-alkane hydroisomerization to their corresponding branched isomers have special interest in the petrochemical industry to increase the gasoline octane number. Thus, the hydroisomerization process serves as a better alternative for producing high performance gasoline suitable for compliance with environmental policies [8]. The alkane hydroisomerization process is carried out over a wide variety of bifunctional catalysts like Pt/Cl/alumina [9], Pt or Pd or Ni on MOR [10–12], ZSM-5 [13], BEA [13,14], FAU [15], FAU/EMT [16], SAPO-11 [13], Pt/HPW/ZrO2 [17], Pt/MCM-22 [18] and Pt/HPW/MCM-41 [19]. Mesoporous materials can be functionalized by impregnation with heteropolyacids ($H_3PW_{12}O_{40}$, $H_3PMo_{12}O_{40}$ and $H_4SiW_{12}O_{40}$) [20,21] and a noble metal like Pt or Pd.

In this work we report the catalytic behavior of bifunctional catalysts in the hydroisomerization of *n*-pentane, where the acid function is given by $H_3PW_{12}O_{40}$ (HPW) and the hydro/dehydrogenating function by Pt or Pd supported on HMS.

2. Experimental

2.1. Catalyst preparation

The mesoporous silica with a wormhole framework structure, denoted HMS, was synthesized via a neutral S°I°, according to pre-

* Corresponding author. Tel.: +58 274 2401371; fax: +58 274 2401286.
E-mail addresses: imbert@ula.ve, freddy.imbert@gmail.com (F. Imbert).
[1] Present address: Seton Hall University, Center for Applied Catalysis, 400 South Orange Avenue, South Orange, NJ 07079, USA.

0920-5861/$ – see front matter © 2011 Elsevier B.V. All rights reserved.
doi:10.1016/j.cattod.2011.04.050

Table 1
Textural properties and metal dispersion of metal-supported catalysts.

Catalyst	BET (m^2/g)	V_P (cm^3/g)	D_p (nm)	Metal dispersion (%)
HMS	746	1.0	2.8	–
Pt/HMS-IS	623	0.9	2.6	27
HPW/Pt/HMS-IS	326	0.5	2.1	–
Pd/HMS-IH	608	0.9	2.5	26
HPW/Pd/HMS-IH	311	0.5	1.8	–

viously reported methods [22]. Dodecylamine (DDA, 9.9 mmol) was dissolved in 10 ml of ethanol, and 85 ml of distilled H_2O was then added to obtain a 89.5:10.5 (v/v) H_2O/EtOH solution of surfactant. The surfactant solution was heated to the desired reaction temperature, and tetraethyl orthosilicate (TEOS) was added to give the following molar composition of the gel: (x) SiO_2:(9.9) DDA:(171) EtOH:(472) H_2O, where x = 2–10. The reaction flask was sealed and stirred at room temperature for 24 h. The resulting solid was filtered out, washed with distilled water, and allowed to air dry at room temperature for 24 h. The surfactant was removed by calcination in air at 600 °C for 4 h, in some cases ethanol extraction was necessary to ensure the complete elimination of surfactant [23].

1 wt.% of Platinum (Pt) was incorporated by solid state ion exchange using $Cl_2Pt(NH_3)_4{\cdot}H_2O$ (PM = 352.12 g/mol, 55–56% Pt, Merck +99) as a precursor. The calcined form of HMS and the Pt salt were mixed in a mortar (20 min slowly followed by 20 min vigorously). The mixture was heated at 2 °C/min up to 500 °C, in a quartz reactor under nitrogen flow (30 ml/min), the catalyst was kept at 500 °C for 2 h [24]. The catalysts prepared by solid state ion exchange were labeled as Pt/HMS-IS. For the palladium (Pd) catalysts, the calcined form of HMS was impregnated using a slight excess of solution required to fill the pore volume of the support with a solution of $Pd(acac)_2$ in toluene in the amount required to obtain 1 wt.% of Pd. The catalyst was dried at 80 °C for 12 h, and calcined in air at 3 °C/min up to 400 °C for 3 h [23]. The catalysts prepared by conventional impregnation were labeled as Pt/HMS-IH.

The preparation of HPW on Pt(or Pd)/HMS was as follows: methanol was added to a given mass of support (10 ml of methanol per g of support), and to this suspension the proper amount of $H_3PW_{12}O_{40}$ was added as to obtain 30 wt.% The suspension was stirred for 18 h at room temperature. Finally, the solvent was evaporated at 60 °C, and the solid dried at 100 °C for 24 h [25]. The solids were labeled as HPW/Pt/HMS-IS and HPW/Pt/HMS-IH. We have chosen a 30 wt.% of HPW because in previous works we have established that the *m*-xylene isomerization and *n*-hexane cracking on HPW/MCM-48 [25] and *n*-pentane hydroisomerization on HPW/Pt/MCM-41 [19] reached the highest conversion at this concentration. Juan et al. [26] have reported similar results for esterification of fatty acid on HPW/Pt/MCM-41.

2.2. Catalyst characterization

Power X-ray diffraction (XRD) measurements were measured using Cu-Kα radiation (λ = 1.542 Å) and a Rigaku X-ray Geigerflex diffractometer equipped with a rotating anode operated at 40 kV and 2 mA. The analysis was carried out from 1 to 20° 2θ, in a scanning continuous mode with a rate of 0.5°/min.

The N_2 adsorption–desorption measurements were performed on a Micromeritics ASAP 2010 apparatus after 4 h evacuation at 623 K and 5×10^{-3} mm Hg. Surface areas (BET) were calculated from a linear part of the BET plot according to IUPAC recommendations. Pore volume and pore diameter (B.J.H.) were determined from the N_2 adsorption branch using the Horvath–Kawazoe model.

Metal dispersion was determined by H_2 chemisorption in an automatic Micromeritics apparatus model ASAP 2010. Hydrogen chemisorption was carried out at 70 °C in the pressure range 1–100 mm Hg. The hydrogen uptake was evaluated from the irreversible amount of absorbed H_2 as determined by the difference between the first (total) and the second (reversible) isotherms.

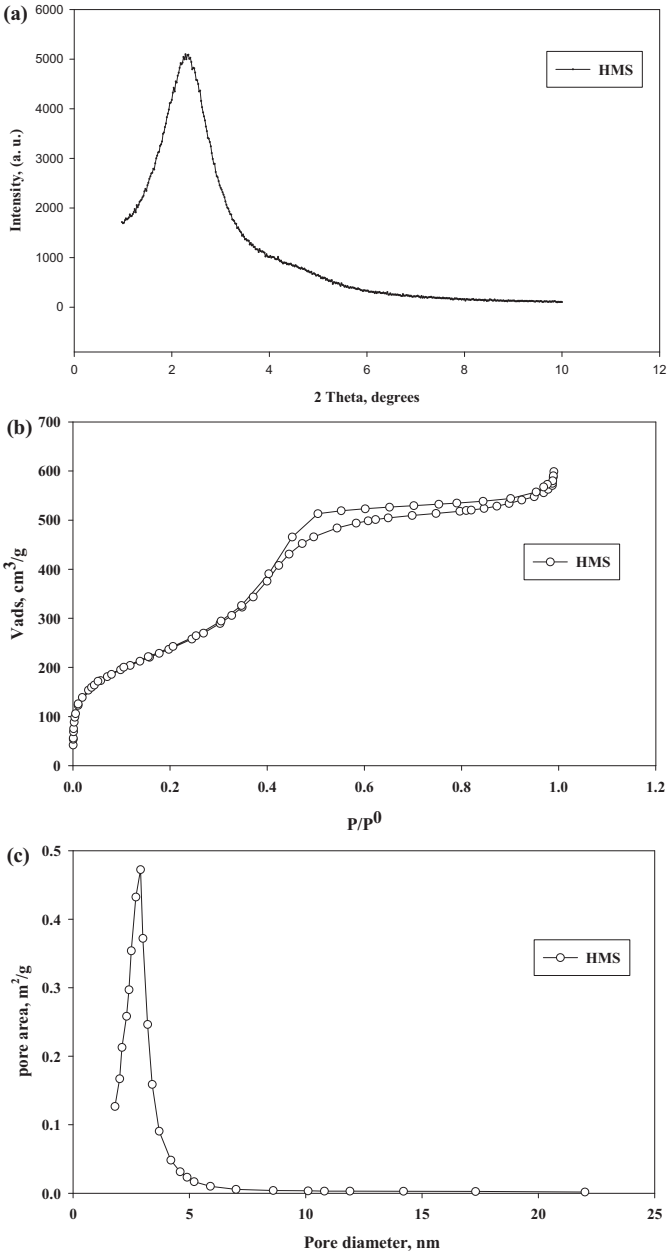

Fig. 1. (a) HMS XRD pattern, (b) adsorption/desorption N_2 isotherm of support type HMS and (c) pore size distribution for the support type HMS.

Scanning electron microscopy (SEM) was performed on a Hitachi S2500, equipped with Kevex energy dispersion X-ray spectrometer, model Delta-3.

The thermogravimetric analysis (TGA) and the differential scanning calorimetry (DSC) experiments were performed on a TA Instruments model SDT Q600. The thermograms were collected from room temperature to 1073 K at 20 K/min under nitrogen flow of 100 ml/min.

2.3. Catalytic experiments

The catalytic reaction was performed in a down flow fixed bed reactor equipped with electric furnace at atmospheric pressure.

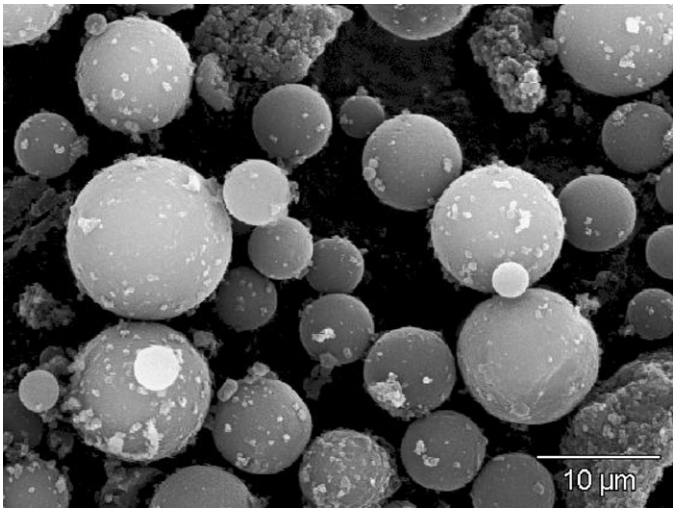

Fig. 2. SEM micrograph of the solid type HMS.

The reaction temperatures were in the range from 200 to 400 °C. A 150 mg portion of the catalyst was packed into the reactor and then activated, *in situ* under H_2 flow (30 ml/min) for 1 h at 200 °C (rate 5 °C/min) previous to the catalytic test. The reaction flow (H_2) was saturated with the reactant *n*-pentane at −3 °C (p° = 158 mm Hg), the H_2/HC ratio and the hydrocarbon molar flow were 3 and 32.6 (mmol/h), respectively. The time on stream (*tos*) was in the range of 2–10 min. The reaction products were analyzed on-line with a gas chromatograph, equipped with FID and capillary column (CHOMPACK Plot 50 m).

3. Results and discussion

3.1. Catalyst characterization

The XRD pattern for HMS silica is presented in Fig. 1a. The wormhole framework of HMS exhibits a single diffraction line at $2\theta = 2.25^\circ$, $d_{100} = 4.5$ nm and $a_o = 5.2$ nm, this indicates the repetitive pattern of the pore distances. This peak at low angles appears common to wormhole pore structures synthesized using a large alkyl chain amine surfactant (S°) [4,22,23]. These materials possess a mesostructure without long-range order, probably due to the weak H-bonding forces, that governs the neutral S°I° assembly process and to the corresponding small scattering domain sizes [4,27]. Fu et al. [28] assigned the observed big peak to a lack of arrangement, due to the weak hydrogen bond, that controls the

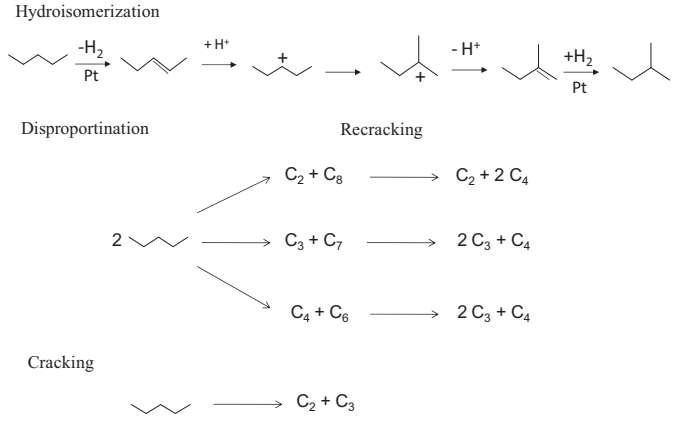

Fig. 3. Reaction diagram for the n-heptane hydroisomerization.

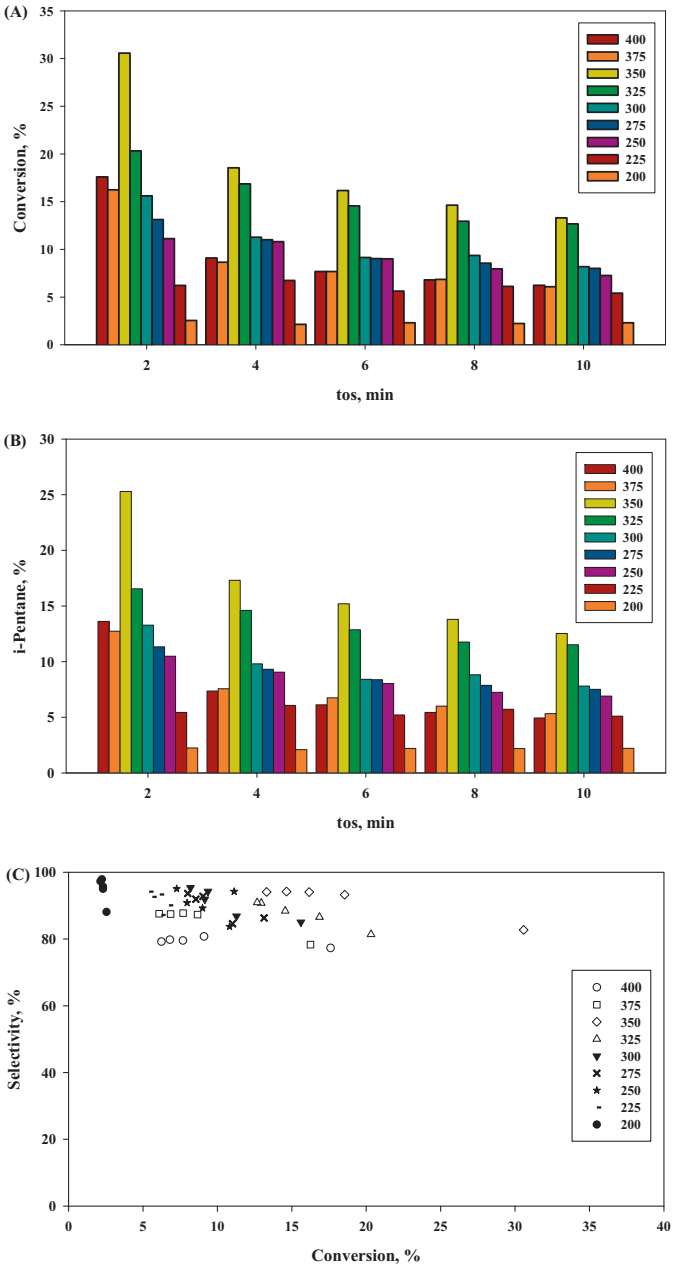

Fig. 4. (a) Conversion (%), (b) *i*-pentane yield (%) and (c) selectivity on HPW/Pt/HMS-IS as function of *tos* (min) at different reaction temperatures.

assemblage in the S°I° mechanism. They reported for a HMS solid a $d_{100} = 3.1$ nm and $a_o = 3.6$ nm. On the other hand, Tanev and Pinnavaia [4], have reported a XRD pattern similar to ours. They have attributed the peak broadening to the poor arrangement order and to the presence of hexagonal pores, from where derived its name (Hexagonal Mesoporous Silica).

The adsorption/desorption N_2 isotherm is type IV (shown in Fig. 1b), which according to the IUPAC is typical of mesopore solids, with a type H1 hysteresis loop characteristic of the capillary condensation in the mesopores. At low relative pressures, the isotherm shows the pores filling in monolayer (0–0.4 P/P°), followed by a steep increase of N_2 adsorption, due to the mesopore progressive filling. The textural properties of the catalysts are summarized in Table 1. The surface areas, as determined by fitting the BET equation to nitrogen adsorption isotherms in the partial pressure region below 0.30, pore size was calculated by B.J.H. equation, and the total pore volume by a single point method at 0.98 P/P°. Zhou et al. [27]

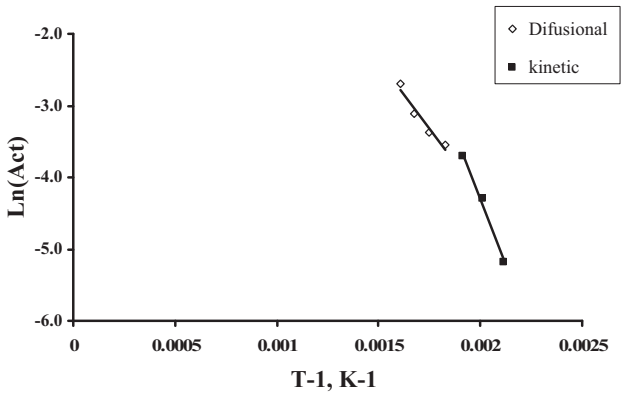

Fig. 5. Arrhenius plot.

have reported the specific surface area (S_{BET}) and the cumulative pore volume for the HMS to be 866 $m^2\ g^{-1}$ and 0.67 $cm^3\ g^{-1}$, respectively. It can be seen that the pore size distribution (see Fig. 1c) is very narrow, centered at 2.8 nm, and the wall thickness was 2.4 nm ($a^\circ - D_p$). The surface area and pore volume of the HMS loaded with Pt and Pd did not decreased so significantly, implying that the Keggin's structure (kinetic diameter = 1.2 nm), should be well dispersed onto the pore diameters of Pd/HMS and Pt/HMS catalysts. The incorporation of both metal and heteropolyacid (HPW) inside the pores seems to cause a decrease of surface area, diameter and volume of pore. The surface area and the pore volume observed for the catalysts were slightly lower than the expected, on the grounds of physical mixture, that may be due to the low contribution of HPW layer formed in side the pores to the total surface area. SEM image (see Fig. 2) show the typical sphere of variable size of the HMS mesophase.

The TGA–DSC profiles showed the presence of four zones or regions corresponding to different processes, as follows: (1) the first, corresponding to the desorption of physisorbed water (non coordinated) between 30 and 100 °C. (2) The second, associated to the loss of crystallization water from the HPW secondary structure (Keggin type anion), in the region of 100–300 °C, and some physisorbed water strongly retained inside the HMS pores. (3) The third, involves two reactions that overlaps: the dehydroxylation (or condensation) of silanol groups and the HPW thermal decomposition (structural water loss), at 300–600 °C. (4) The fourth between 600 and 800 °C due to the lost of structural water from the stabilized HPW (by the formation of surface aggregates) and sublimation of oxides such as WO_3 and P_2O_5. The TGA was run up to 800 °C only for the HPW, and to 600 °C for the supported catalysts. A summary of TGA–DSC results is presented in Table 2.

While HPW weight loss, in the range of 300–600 °C, is associated to its decomposition to $PW_{12}O_{38.5} + H_2O$. For the HPW/Pt/HMS-IS or HPW/Pd/HMS-IH catalysts, the weight loss is determined mainly by silanol groups, since their values are greater than for HPW, but lower than for HMS. The interaction between $H_3PW_{12}O_{40}$ at low loadings and surface silanol groups (Si–OH) has been detected by ^1H, ^{31}P MAS NMR and Raman spectroscopy for SiO_2 and MCM-41 [21].

3.2. Catalytic activity and selectivity

In a previous work, we show that the activity and selectivity for the *n*-pentane hydroisomerization [19] and in the *m*-xylene isomerization [25] at fixed temperature on HPW supported on MCM-41 and MCM-48 mesostructured materials, are strongly influenced by the concentration of heteropolyacid (HPW) used. We have found a maximum activity for the catalysts containing 30 wt.% HPW [19,25]. A similar result was reported by Juan et al. [26] for esterification of fatty acid on HPW supported on MCM-41. Thus, the optimal HPW loading of 30 wt.% was chosen for further studies on mesoporous structures. Noble metals are considered very efficient in activation of hydrogen and suppressing the coke formation in hydrocarbon treatment processes over dual function catalysts. The noble metals are proposed to activate hydrogen and spillover hydrogen to the acidic sites. Without noble metals, the catalyst usually loses activity due to severe coking formation on the acidic sites. In general the alkanes are presumably activated by dehydrogenation, and the resultant alkenes are isomerized on Bronsted acidic centers (see Fig. 3). Because alkenes are much more basic than alkanes, they can be protonated by moderately strong Bronsted acid centers of the heteropolyacid phase. In some cases the interaction between the heteropolyacid and hydroxyl groups present in the mesoporous silica is essential; the degree of dispersion will influence the acid strength of these sites.

Fig. 4a and b shows the conversion and selectivity as function of time on stream (*tos*, min), and Fig. 4c shows selectivity to *i*-pentane as function of conversion, at different temperatures for the HPW/Pt/HMS-IS catalyst. The catalyst activity increased as the temperature increased from 200 up to 350 °C, as expected for an activated process; however, for higher temperatures (375 and 400 °C) the activity drops, probably because the HPW decompose to H_2O and $PW_{12}O_{38.5}$, in the range of 300–600 °C, as we have shown by TGA–DSC and TPD, and it has been reported elsewhere [25,29]. Both conversion and *i*-pentane yield showed maximum at a reaction temperature of 350 °C.

The Arrhenius plot (see Fig. 5) was calculated from the data obtained at the shortest experimental *tos*, 2 min. Using the Arrhenius plot the apparent activation energies were calculated for the diffusional (Ea (Diff) = 7.5 kcal/mol) and kinetic (Ea (Kin) = 15.2 kcal/mol) regimes for *n*-pentane hydroisomerization reaction on HPW/Pt/HMS-IS catalyst. The latter compares quite well with the value of 20.97 kcal/mol, reported for this reaction on Pt/BEA (Si/Al = 14 and 1.5 wt.% Pt) [14] and 17 kcal/mol reported for dehydroisomerization on Pt/SAPO-11 for the temperature range 250–300 °C [30]; however is lower than 27 kcal/mol found for Pt-HMOR catalysts in similar conditions [12] and a value of 35 kcal/mol [31] reported for Pt/HMordenite, for 180–220 °C, total pressure of 30 bar and a H_2/HC = 2. It has been found that *n*-pentane isomerization on Pt/BEA (Si/Al = 14 and 1.5 wt.% Pt) requires at least a temperature > 250 °C [14], whereas in the present work the reaction starts from 200 °C on HPW/Pt/HMS; therefore, the latter catalyst has stronger acid sites.

As a function of *tos* the activity decreased. This may occur due to some coke formation and, in the case of high temperatures, also due to metal sintering and/or some acid decomposition. The selec-

Table 2
TGA weight loss (ΔP%) data of support and catalysts.

Catalyst	ΔP_1 (%) (30–100 °C)	ΔP_2 (%) (100–300 °C)	ΔP_3 (%) (300–600 °C)	ΔP_4 (%) (600–800 °C)
HPW	5.11	3.31	0.64	0.85
HMS	8.11	0.84	1.90	–
HPW/Pt/HMS-IS	13.34	1.92	1.23	–
HPW/Pd/HMS-IH	4.00	1.88	1.44	–

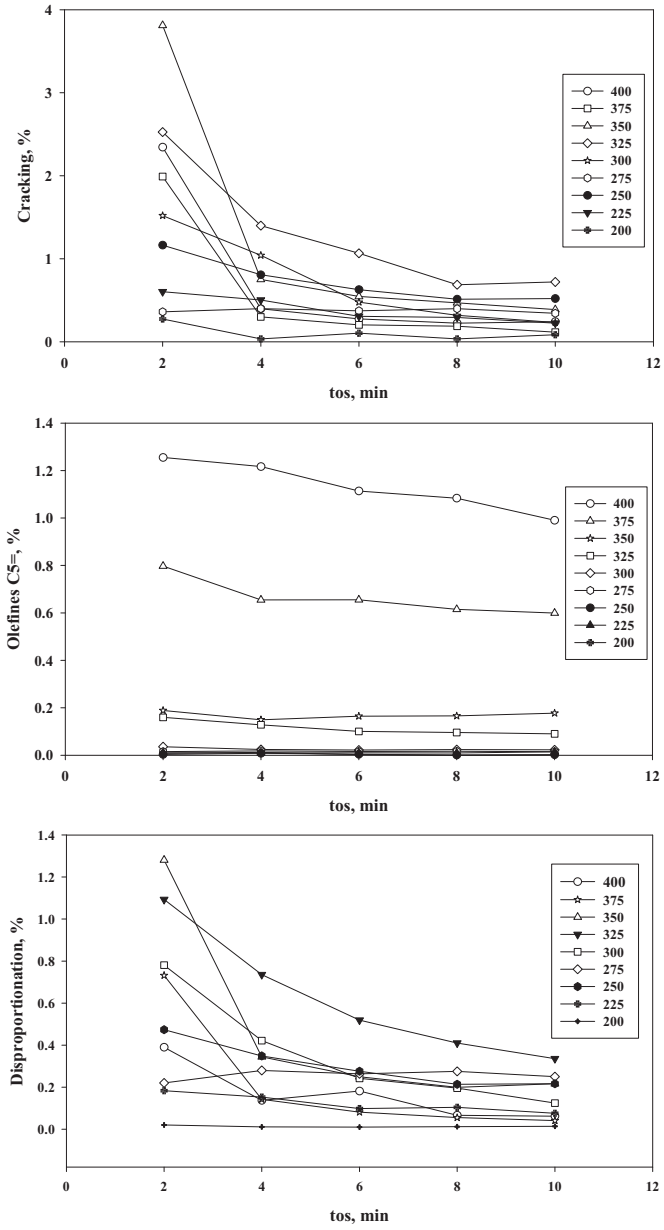

Fig. 6. Secondary reactions on HPW/Pt/HMS-IS, as function of *tos* (min) at different reaction temperatures: cracking (%), dehydrogenation (%) and disproportionation (%).

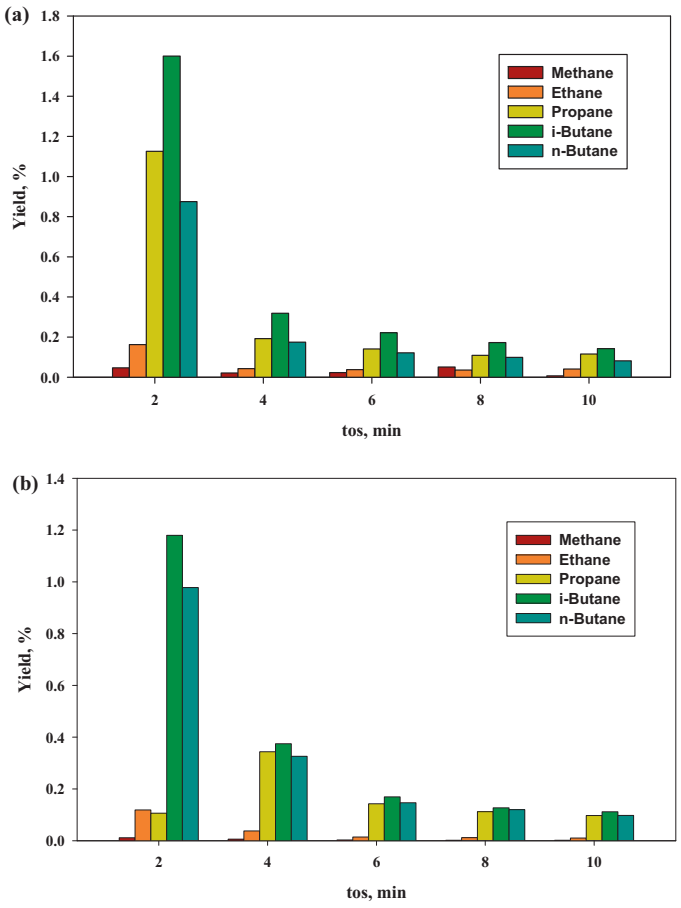

Fig. 7. Cracking product distribution on (a) HPW/Pt/HMS-IS and (b) HPW/Pd/HMS-IH.

tivity toward *i*-pentane was quite high even for high temperature as 400 °C. It can be seen in Fig. 4c that, as catalyst deactivated the selectivity increased, indicating that the cause of deactivation affected mostly the acid sites responsible for the formation of minor products.

Besides *i*-pentane, the main product, other minor products were observed, mainly C_1–C_4, which probably come from cracking and product recracking (<4%) (see Fig. 3 for the reaction scheme), $C_6^=$, which come from *n*-pentane dehydrogenation (<1.3%) (Fig. 6) and products with carbon number greater than five, that may come from *n*-pentane disproportionation (<1.3%) (Fig. 6), a similar product distribution was observed on Pt/FAU/EMT [16]. The by-products are considered to be formed by β-scission of intermediates on acid sites, and not by the hydrogenolysis of *n*-pentane on metallic sites. Thus, the acidic properties of the catalyst, particularly the acid strength, are considered to be a critical factor determining the selectivity. Both cracking and disproportionation yields as function of *tos* showed a similar behavior, as can be seen in Fig. 7, which shows how dramatically the cracking and disproportionation yields fall as function of *tos*, this marked deactivation may be caused by coke formation. Dehydrogenation yield increased with temperature and appeared to be less affected by deactivation. The yields of these secondary reactions were in the following order: cracking > dehydrogenation ≥ disproportionation. Fig. 7 shows the typical cracking product distribution [16] for these catalysts. The major component is i-butane, while CH_4 and C_2H_6 are present at trace level, indicating that the hydrogenolysis reaction is practically insignificant, and that C_3 and C_4 must come from recracking of dimerization or disproportionation products.

The effect of the nature of the hydro/dehydrogenating sites is shown in Fig. 8, where the Pt and Pd catalysts are compared. It clearly illustrates that Pt catalyst was more active and selective than the Pd catalyst. Elangovan et al. [32] for isomerization and hydrocracking of n-decane on MCM-41, and Lee and Rhee [33] for *n*-hexane isomerization on β zeolite reported similar results.

Table 3
Chemical analysis obtained from EDX data.

Catalyst	Si (wt.%)	W (wt.%)	Pt (wt.%)	Pd (wt.%)	W/Si (w/w)	Metal/W (w/w)	HPW (wt.%)
HPW/Pd/HMS-IH	33.8	23.8	–	0.79	0.70	0.033	31
HPW/Pt/HMS-IS	37.9	22.4	1.27	–	0.59	0.057	29

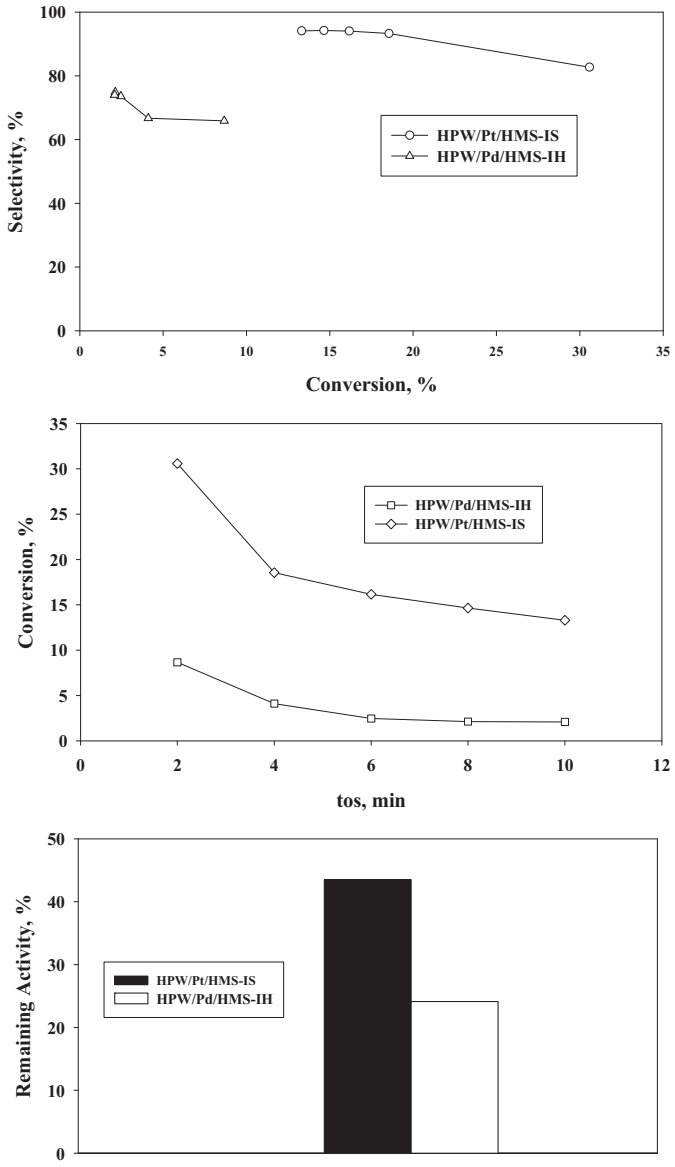

Fig. 8. Comparison of *n*-pentane conversion (%) at 350 °C, on HPW/Pt/HMS-IS and HPW/Pd/HMS-IH.

The higher Pt activity is associated to its electronic configuration ($5d^9 6s^1$), which needs an electron to complete its *d* orbital; while Pd already has its last orbital complete ($4d^{10}$). The catalytic stability (defined as the ratio of activity at 10 min respect to activity at 2 min) also was higher for Pt catalyst (see Fig. 8), this can be attributed to its hydrogenating power that inhibited the coke formation. When comparing the two catalysts, the activity–structure correlation was observed. Pt catalyst was more active than Pd catalyst, in our case, because the amounts of Pt (1.27 wt.%) and the ratio metal to acid (0.057, w/w) were higher than those of Pd catalyst (0.79 wt.% and 0.033, w/w, respectively) (see Table 3).

4. Conclusions

The HPW Keggin structure was retained and well dispersed inside the HMS pores. Both catalysts were very active and selective for *n*-pentane hydroisomerization to *i*-pentane. The optimum temperature for HPW/Pt/HMS-IS (30 wt.% HPW, 1.3 wt.% Pt) was 350 °C, with a selectivity of 78–98%. At higher temperatures (375 and 400 °C) the activity decreases, because the HPW decomposes. The yields of the minor reactions (<6%) were in the following order: cracking > dehydrogenation ≥ disproportionation.

The catalysts suffer a fast deactivation during the reaction. The amount of acid sites decreased during on-stream conditions, as deduced from decrease in the selectivity toward cracking and disproportion products. As a consequence, the selectivity toward *i*-pentane increased. The deactivation during *tos* affected mainly the acid sites responsible for the cracking and disproportionation reactions, thus the selectivity to *i*-pentane increased. The bifunctional Pt/HPW catalyst was more effective than Pd/HPW supported on HMS catalyst.

Acknowledgements

The authors are grateful to CDCHT of the Universidad de Los Andes for its financial support through the project C-1385-06-08-ED and to the Electronic Microscopy Laboratory (LAQUEM) of the Science Faculty of Universidad de Los Andes.

References

[1] T. Yanagisawa, T. Shimizu, K. Kuroda, C. Kato, Bull. Chem. Soc. Jpn. 63 (1990) 988–992.
[2] C. Kresge, M. Leonowicz, W. Roth, J. Vartuli, J. Beck, Nature 359 (1992) 710–712.
[3] J. Beck, J. Vartuli, W. Roth, M. Leeonowicz, C. Kresge, K. Schmitt, D. Olson, E. Sheppard, S. McCullen, J. Higgins, L. Schlenker, J. Am. Chem. Soc. 114 (1992) 10834–10843.
[4] P. Tanev, T. Pinnavaia, Science 267 (1995) 865–867.
[5] S. Bagshaw, E. Prouzet, T. Pinnavaia, Science 269 (1995) 1242–1244.
[6] D. Zhao, Y. Wan, The synthesis of mesoporous molecular sieves, in: J. Cejka, H. van Bekkum, A. Corma, F. Schüth (Eds.), Introduction to Zeolite Science and Practice, 3rd ed., Elsevier, Amsterdam, 2007, pp. 241–300.
[7] R. Xu, W. Pang, J. Yu, Q. Huo, J. Chen, Chemistry of Zeolites and Related Porous Materials: Synthesis and Structure, Wiley & Sons (Asia), Singapore, 2007.
[8] A. Galadima, J.A. Anderson, R.P.K. Wells, Sci. World J. 4 (3) (2009) 15.
[9] A. Corma, A. Martínez, The chemistry of catalytic processes, in: M. Guisnet, J.-P. Gilson (Eds.), Zeolite for Cleaner Technologies, Imperial College Press, London, 2002, pp. 29–55.
[10] L.O. Almanza, T. Narbeshuber, P. dÁraujo, C. Naccache, Y.B. Taarit, Appl. Catal. A: Gen. 178 (1) (1999) 39–47.
[11] D. Karthikeyan, N. Lingappan, B. Siv asankar, N. Jabarathinam, Appl. Catal. A: Gen. 345 (1) (2008) 18–27.
[12] F. Aguirre, Hidroisomerización de n-pentano sobre zeolita tipo Pt-HMOR, Trabajo Especial de Grado (Undergraduate Spetial work for the Degree), Universidad de Los Andes, 2006.
[13] C.M. López, Y. Guillén, L. García, L. Gómez, A. Ramírez, Catal. Lett. 122 (2008) 267–273.
[14] E. Sosa, P. Rodríguez, F. Aguirre, L. Belandría, A. Uzcátegui, G. González, F. Imbert, Avances en Química 4 (1) (2009) 25–36.
[15] T.D. Pope, J.F. Kriz, M. Stanciulescu, J. Monnier, Appl. Catal. A: Gen. 233 (2002) 45–62.
[16] L.N. Belandría, C.S. Gonzàlez, F. Aguirre, E. Sosa, A. Uzcátegui, G. González, J. Brito, S.L. González-Cortés, F.E. Imbert, J. Mol. Catal. A: Chem. 281 (2008) 164–172.
[17] A.V. Ivanov, T.V. Vasina, V.D. Nissenbaum, L.M. Kustov, M.N. Timofeeva, J.I. Houzvicka, Appl. Catal. A: Gen. 259 (2004) 65–72.
[18] A. Martins, J.M. Silva, F.R. Ribeiro, M. Guisnet, M.F. Ribeiro, Stud. Surf. Sci. Catal. 174 (2) (2008) 1135–1138.
[19] L.N. Belandria Rodríguez, E. Garcia, J. Rondón, F.E. Imbert, A.A. Uzcátegui Paredes, M.d'L. Villarroel Mejías, M. Marín, Avances en Química 5 (1) (2010) 67–71.
[20] M.T. Pope, Heteropoly and Isopoly Oxometalates, Springer Verlag, Berlin, 1969.
[21] I.V. Kozhevnikov, Chem. Rev. 98 (1) (1998) 171–198.
[22] P.T. Tanev, T.J. Pinnavaia, Chem. Mater. 8 (1996) 2068–2079.
[23] M. Marín, PhD Thesis, Universidad de Concepción, Chile, 2004.
[24] L. Belandria, Trabajo Especial de Grado (Undergraduate Special Work for the Degree), Universidad de los Andes, Venezuela, 2005.
[25] E. García, P. Rodríguez, A. Lobo, P. Hoffman, Á. Uzcategui, M. Villarroel, H. Del Castillo, S. González Cortes, F.E. Imbert, Avances en Química 5 (2) (2010) 99–105.
[26] J.Ch. Juan, J. Zhang, M.A. Yarmo, J. Mol. Catal. A: Chem. 267 (1–2) (2007) 265–271.
[27] R. Zhou, Y. Cao, S. Yana, J. Deng, Y. Liao, B. Hong, Catal. Lett. 75 (1–2) (2001) 107–112.
[28] Z. Fu, J. Chen, D. Yin, L. Zhang, Y. Zhang, Catal. Lett. 66 (2000) 105–108.
[29] P.A. Jalil, M.A. Al-Daous, A-R.A. Al Arfaj, A.M. Al-Amer, J. Beltramini, S.A.I. Barri, Appl. Catal. A: Gen. 207 (1–2) (2001) 159–171.
[30] G. Herrera, D. Lardizábal, V. Collins, Catal. Lett. 76 (3–4) (2001) 161–166.
[31] A. Holló, J. Hancsók, D. Kalló, Appl. Catal. A: Gen. 229 (2002) 93–102.
[32] S. Elangovan, C. Bischof, M. Hartmann, Catal. Lett. 80 (2002) 38–40.
[33] J. Lee, H. Rhee, J. Catal. 177 (1998) 208–216.